Modeling the Atmospheric General Circulation Using a Spherical Geodesic Grid: A New Class of Dynamical Cores

Todd D. Ringler
Ross P. Heikes
David A. Randall

Department of Atmospheric Science
Colorado State University
Fort Collins, Colorado

NCAR CGD Seminar Series
May 6, 1999

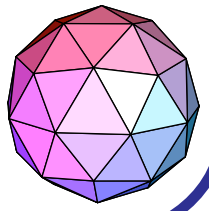

OUTLINE

I. Description of a spherical geodesic grid

II. Continuous equations

III. Discretization on the geodesic grid

IV. Held-Suarez Test Case results

V. Preliminary AGCM results

VI. Conclusions

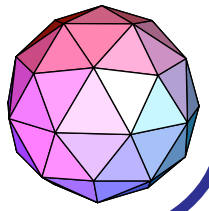

What are we looking for in a grid?

1) Homogeneity

2) Isotropy

3) Capability to increase resolution sufficient to resolve scales of interest

4) Allows the implementation of accurate finite-difference stencils

5) Allows the formulation of conservative finite-difference schemes

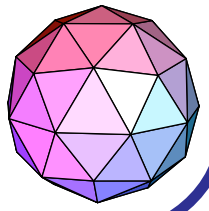

The Starting Point of a Spherical Geodesic Grid

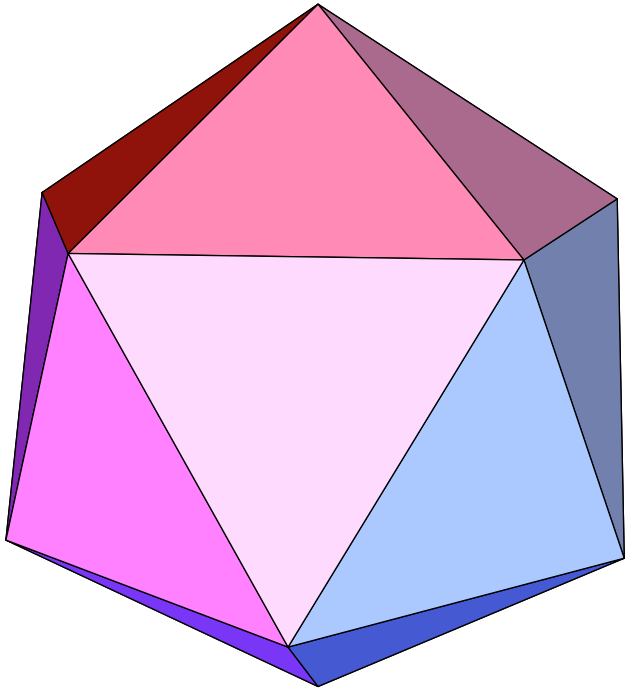

Regular Icosahedron

- Inscribed in a unit sphere
- 20 triangular faces
- 12 vertices

Each vertex will be associated with a grid point.

Generating Geodesic Grids with Higher Resolution

the method of recursive bisection and projection

a regular icosahedron

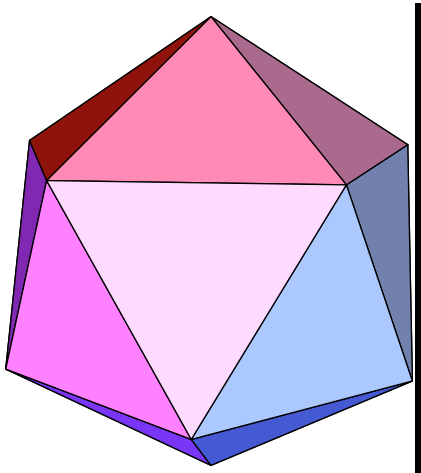

bisect each face

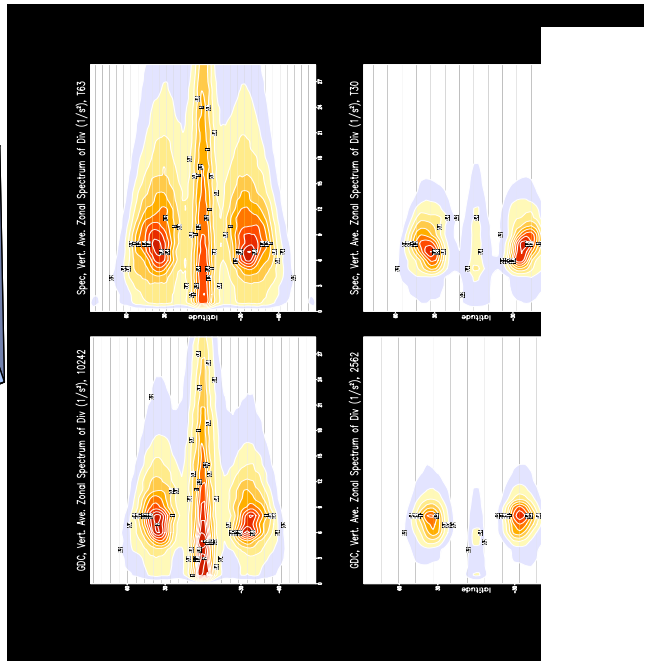

project each new vertex to the unit sphere

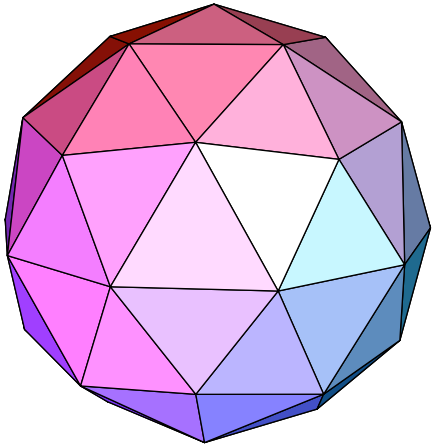

.... and so on until we reach our target resolution

42 vertices

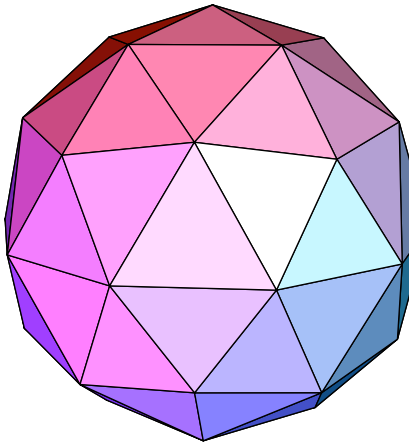

162 vertices

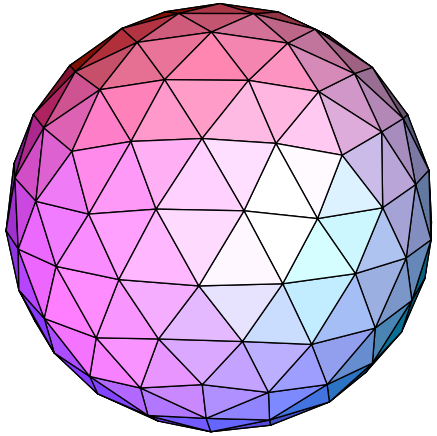

642 vertices

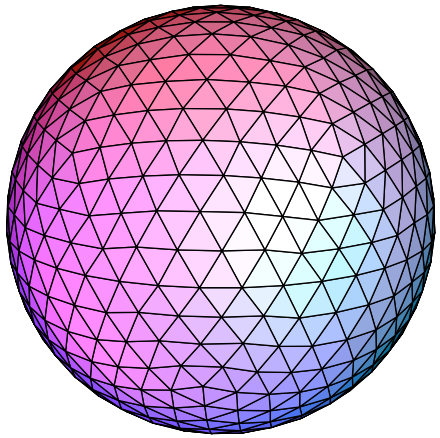

Our target resolution is 10242 grid points.

Assigning an Area to each Vertex

The area associated with grid point P_0 is the set off all points closer to P_0 than any other grid point.

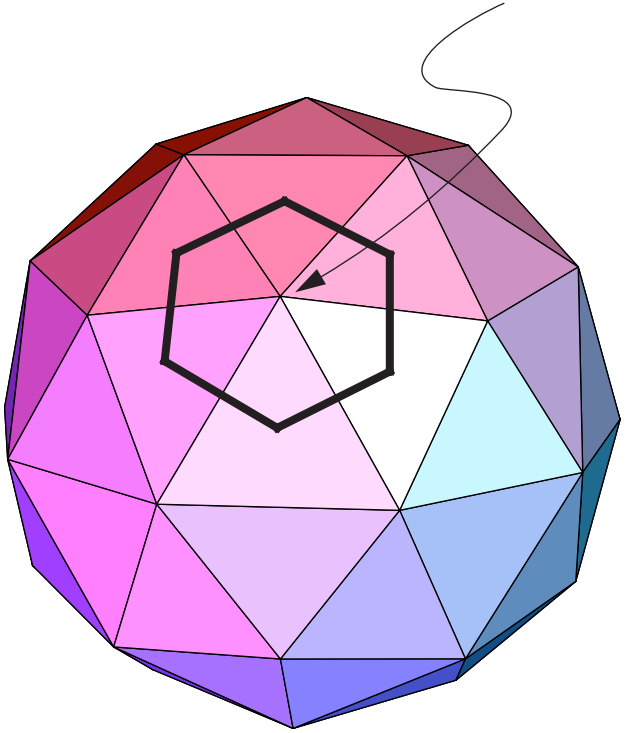

All of the resulting grid cells are hexagons, except for 12 pentagons.

The centers of the 12 pentagons are the 12 vertices of the initial icosahedron.

Properties of the geodesic grids at different resolution

R	Number of cells N_c	Number of cells along equator	Average cell area in km^2	Ratio of smallest cell to largest cell	Average distance between cell centers in km	Ratio of smallest to largest distance btn cell centers
0	42	10	1.21e7	0.885	3717.4	0.881
1	162	20	3.14e6	0.916	1909.5	0.820
2	642	40	7.94e5	0.942	961.6	0.799
3	2562	80	1.99e5	0.948	481.6	0.790
4	10242	160	4.98e4	0.951	240.9	0.789
5	40962	320	1.24e4	0.952	120.5	0.788

$$N_c = 5 \cdot 2^{2R+3} + 2 \quad ; \quad R \geq -1$$

AMIP2 SST on geodesic grid with 10242 grid cells

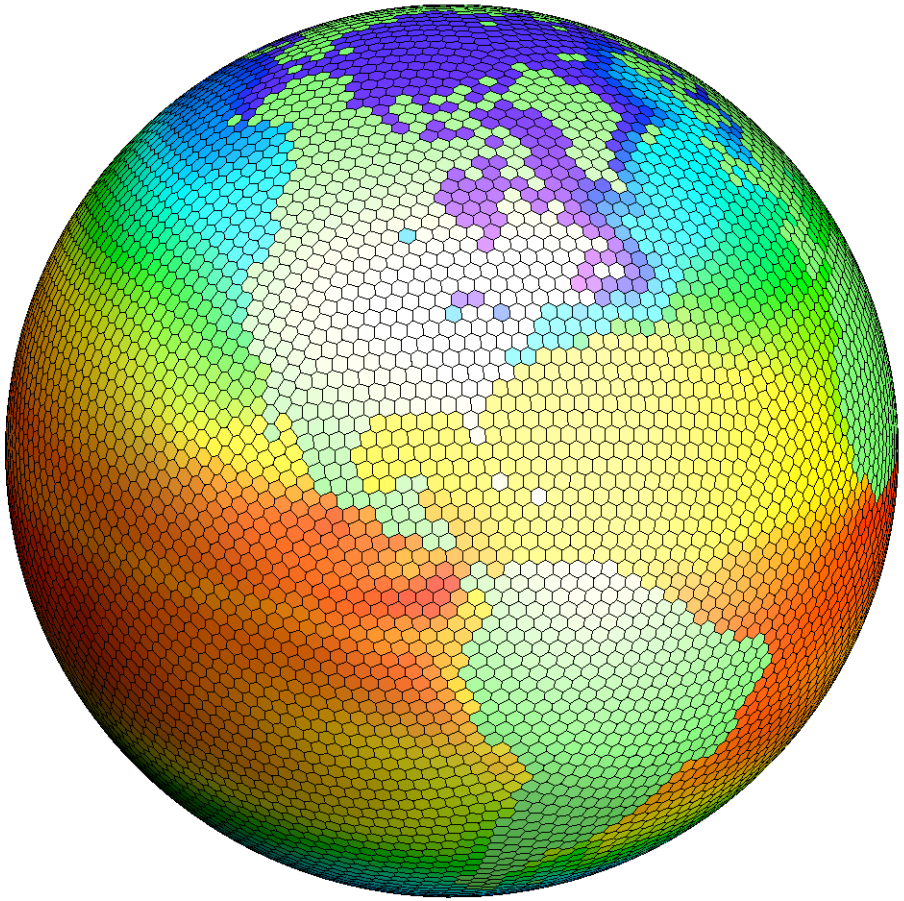

Spherical Geodesic Grids have been around for awhile...

Williamson (1968) Sadourny, Arakawa, and Mintz (1968)	barotropic vorticity equation; several day integrations
Sadourny and Morel (1969) Williamson (1969)	shallow water equations, β-plane
Masuda and Ohnishi (1986)	formulated the vorticity-divergence equations on a spherical geodesic grid
Heikes and Randall (1995a,b)	shallow water equations on a sphere, developed efficient elliptic solver

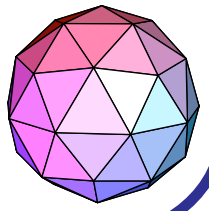

The continuous form of the Primitive Equations

Momentum:
$$\frac{\partial}{\partial t}\underset{\sim}{V} + \left(\frac{\zeta + f}{\pi}\right)\underset{\sim}{k} \times \pi\underset{\sim}{V} + \nabla K + \dot{\sigma}\frac{\partial}{\partial \sigma}\underset{\sim}{V} = -\nabla_p \Phi + \underset{\sim}{G}$$

Potential Temperature:
$$\frac{\partial}{\partial t}(\pi\theta) + \nabla\bullet(\pi\theta\underset{\sim}{V}) + \frac{\partial}{\partial \sigma}(\dot{\sigma}\pi\theta) = \frac{\pi\theta Q}{c_p T}$$

Tracers:
$$\frac{\partial}{\partial t}(\pi q) + \nabla\bullet(\pi q\underset{\sim}{V}) + \frac{\partial}{\partial \sigma}(\dot{\sigma}\pi q) = S$$

Surface Pressure:
$$\frac{\partial p_s}{\partial t} = \int_{\sigma=0}^{\sigma=1} -\nabla\bullet(\pi\underset{\sim}{V})\partial\sigma$$

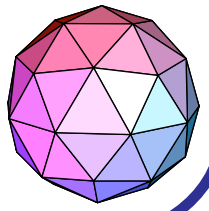

The Vorticity-Divergence Form of the Governing Equations

Decomposing the velocity field into its rotational and divergent components

$$\underset{\sim}{V} = \underset{\sim}{k} \times \nabla\psi + \nabla\chi$$

Taking the curl and divergence of momentum equation

$$\frac{\partial \eta}{\partial t} - J(\eta, \psi) + F(\eta, \chi) + F\left(\dot{\sigma}, \frac{\partial \psi}{\partial \sigma}\right) + J\left(\dot{\sigma}, \frac{\partial \chi}{\partial \sigma}\right) + J(\sigma\alpha, \pi) = \underset{\sim}{k} \bullet \nabla \times \underset{\sim}{G}$$

$$\frac{\partial \delta}{\partial t} - J(\eta, \chi) - F(\eta, \psi) + F\left(\dot{\sigma}, \frac{\partial \chi}{\partial \sigma}\right) - J\left(\dot{\sigma}, \frac{\partial \psi}{\partial \sigma}\right) + L(K + \Phi) + F(\sigma\alpha, \pi) = \nabla \bullet \underset{\sim}{G}$$

$$J(A, B) = \underset{\sim}{k} \cdot (\nabla A \times \nabla B), \quad F(A, B) = \nabla \bullet (A \nabla B), \quad L(A) = \nabla^2 A$$

$$\psi = \nabla^{-2}(\eta - f), \quad \chi = \nabla^{-2}\delta$$

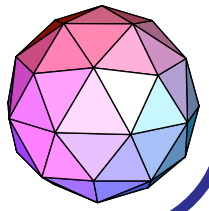

Discretizing the Jacobian on the Spherical Geodesic Grid

Approximation

$$J(\alpha, \beta)\big|_{P_0} \approx \frac{1}{A_c}\iint_{A_c} J(\alpha, \beta)\, dA$$

Conversion

$$\frac{1}{A_c}\iint_{A_c} J(\alpha, \beta)\, dA = \frac{1}{A_c}\oint_{C} \alpha \frac{\partial \beta}{\partial s}\, ds$$

Discrete Approximation

$$\frac{1}{A_c}\left(\oint_{C} \alpha \frac{\partial \beta}{\partial s}\, ds\right) \approx \frac{1}{A_c}\sum_{i=1}^{N} \left(\frac{\alpha_0 + \alpha_i}{2}\right)\left(\frac{b_i - b_{i-1}}{l_i}\right) l_i$$

Reduction

$$J(\alpha, \beta)\big|_{P_0} \approx \frac{1}{6A_c}\sum_{i=1}^{N} (\alpha_0 + \alpha_i)(\beta_{i-1} - \beta_{i+1})$$

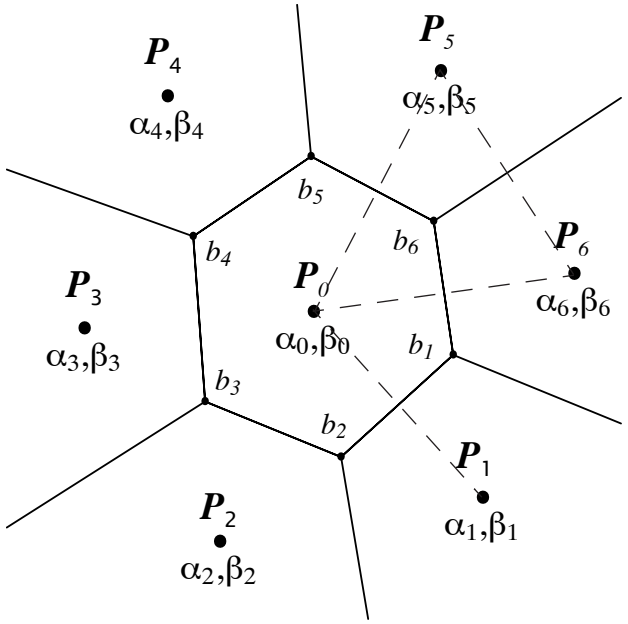

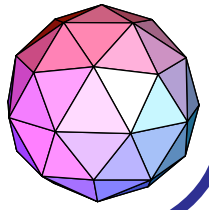

Properties of the Analytic and Discrete Operators

$$\iint_A J(\alpha,\beta)\,dA = 0\,,\ \iint_A F(\alpha,\beta)\,dA = 0\,,\ \text{and}\ \iint_A L(\alpha)\,dA = 0$$

$$\sum_{c=1}^{N_c} A_c \cdot J(\alpha,\beta)\big|_c = 0\,,\ \sum_{c=1}^{N_c} A_c \cdot F(\alpha,\beta)\big|_c = 0\,,\ \text{and}\ \sum_{c=1}^{N_c} A_c \cdot L(\alpha)\big|_c = 0$$

in purely rotational flow, KE and enstrophy are also conserved

$$\iint_A \alpha J(\alpha,\beta)\,dA = 0\ \text{and}\ \sum_{c=1}^{N_c} A_c \cdot \alpha J(\alpha,\beta)\big|_c = 0$$

The discrete operators are second-order accurate.

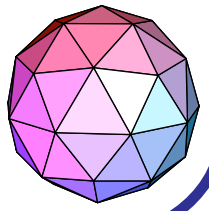

Why use the vorticity-divergence form of the governing equations?

Scalars are preferred to vectors

Conservation issues related to potential vorticity and enstrophy

Z-grid and geostrophic adjustment (Randall 1994)

Isolate terms related to gravity wave propagation

Why not?

inverting elliptic equations in physical space (Heikes and Randall 1995a)

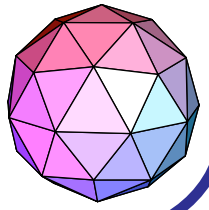

Held-Suarez Test Case (1994)

Boundary Conditions
- flat surface

Forcing
- zonally-symmetric
- restoring to Radiative Equilibrium
- surface Rayleigh friction

Initial Conditions
- isothermal atmosphere at rest + noise

Experiment Specifics
- resolution using 10242 / 2562 grid cells
- integration length of 600 / 1200 days
- time step of 20 / 30 minutes

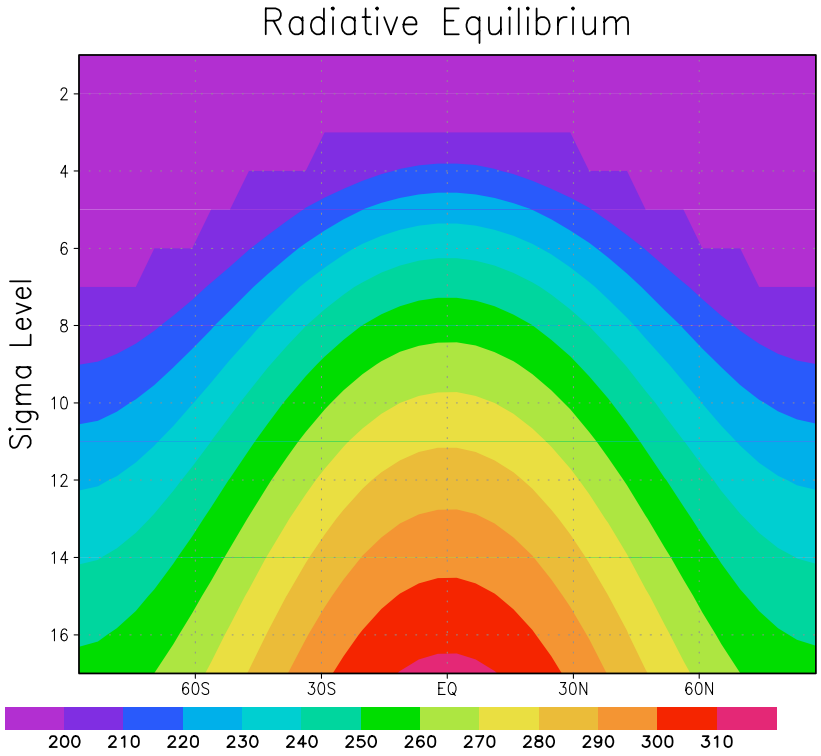

Compare to a Spectral Dynamical Core at T63 / T30 (I. Held)

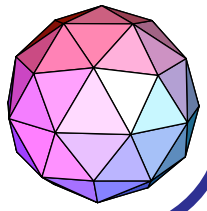

Snapshot of Geodesic Dynamical Core (GDC) model state day 225; 10242

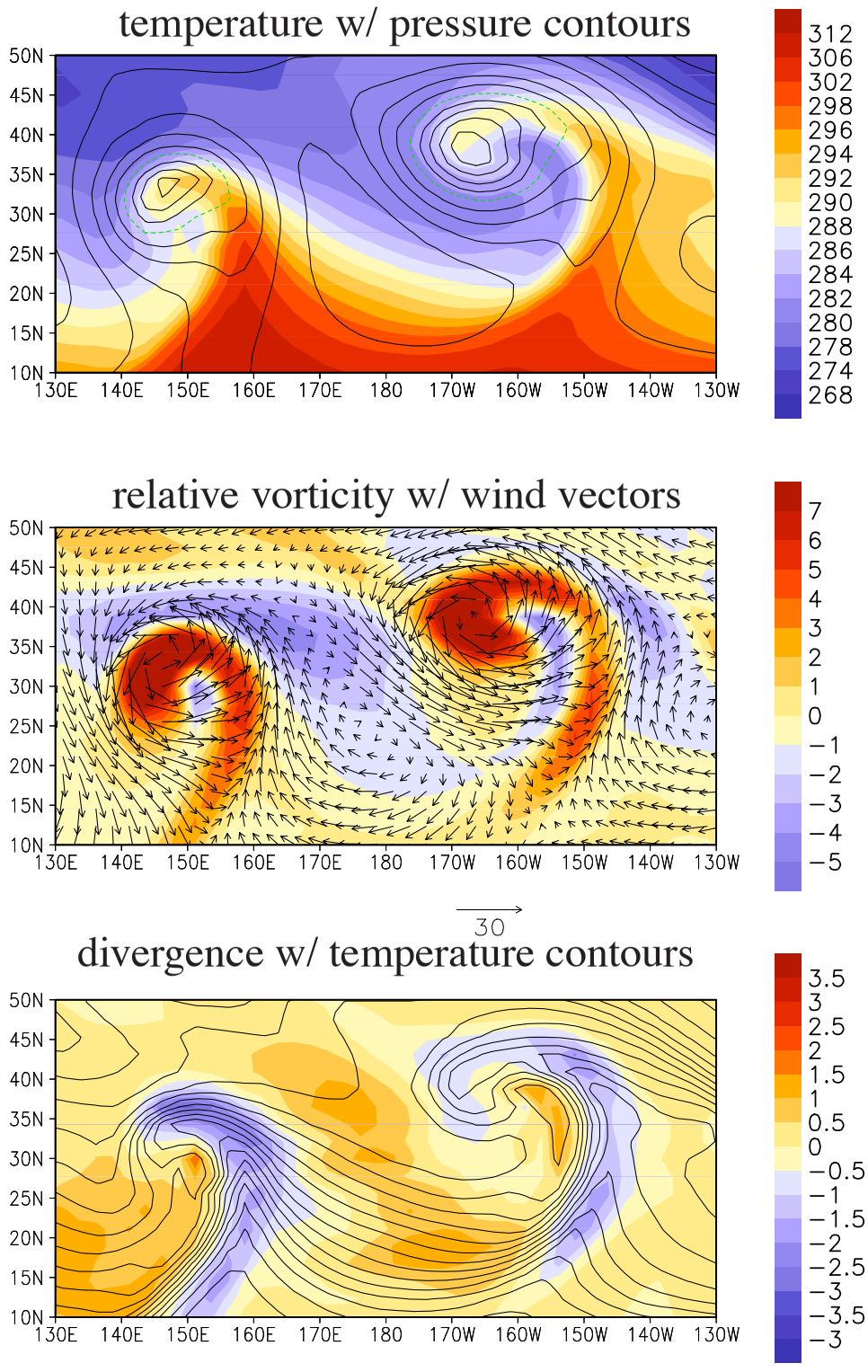

Computational Efficiency

single thread on O2K

Model	Res.	time step (min)	Mflop rate	CPU time (sec) per simulated day
GDC	10242	20	106.0	490.3
GDC	2562	30	91.2	65.7
SDC	T63	20	67.9	411.9
SDC	T30	30	94.3	25.7

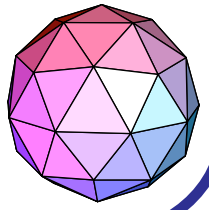

Physical Parameterizations in the CSU AGCM

Radiation from Harshvardhan et al. (1989)

Cloud Microphysics from Fowler et al. (1996)

Cumulus Mass Flux Parameterization from Ding and Randall (1998)

SiB2 Land-Surface Parameterization from Sellers et al. (1996)

PBL parameterization from Suarez et al. (1983)

These parameterizations were not altered when merged with the GDC.
All of these parameterizations are descretized on the geodesic grid.

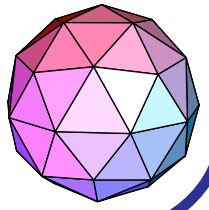

Preliminary GDC/GCM Results

Atmosphere initial condition was a dry isothermal atmosphere at rest

Interpolated Sib2 initial conditions from a lat/lon integration

Simulated 2 years at 2562/17

Interpolated atmospheric state to 10242/17

Simulated 1 year at 10242/17

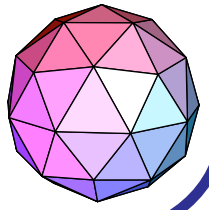

Accomplishments

Built a dynamical core based on a spherical geodesic grid

- combines positive attributes of both traditional spectral models and conventional finite-difference models
- competitive in terms of CPU, gets cheaper everyday

Merged the GDC with the CSU Physics Package

- substantial improvement over previous CSU AGCM results
- deficiencies notwithstanding, reasonable job of simulating the atmospheric climate

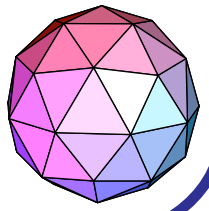

Conclusions and Future Work

Using spherical geodesic grids is a viable methodology

Potential to become the preferred modeling framework

Applications of this grid system in other arenas
- Data Analysis
- Ocean GCM Modeling

Further shake-down of AGCM, AMIP integrations, coupled model simulations

Higher-order stencils

Massively parallel

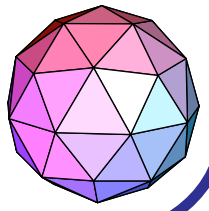

Semi-implicit time stepping scheme

$$\frac{\partial \delta}{\partial t} - J(\eta, \chi) - \nabla\bullet(\eta\nabla\psi) + \nabla\bullet\left(\dot{\sigma}\frac{\partial \chi}{\partial \sigma}\right) - J\left(\dot{\sigma}, \frac{\partial \psi}{\partial \sigma}\right) + \nabla^2 K + \underline{\nabla^2\Phi} + \underline{\nabla\bullet(\sigma\alpha\nabla\pi)} = \nabla\bullet\underset{\sim}{G}$$

$$\frac{\partial p_S}{\partial t} = \int_{\sigma=-1}^{\sigma=2} [J(\pi, \psi) - \underline{\nabla\bullet(\pi\nabla\chi)}]d\sigma'$$

$$\frac{\partial}{\partial t}(\pi\theta) - J(\pi\theta, \psi) + \underline{\nabla\bullet(\pi\theta\nabla\chi)} + \underline{\frac{\partial}{\partial \sigma}(\dot{\sigma}\pi\theta)} = \frac{\pi\theta\underset{\sim}{Q}}{c_p T}$$

$$\partial\Phi = -\alpha\pi\partial\sigma$$

$$(\pi\dot{\sigma})|_{\sigma=\sigma'} = -\sigma'\frac{\partial \pi}{\partial t} + \int_{\sigma=1}^{\sigma=\sigma'} [J(\pi, \psi) - \nabla\bullet(\pi\nabla\chi)]\partial\sigma$$

$$\chi = \nabla^{-2}\delta$$